Research in Astronomy and Astrophysics, 25:011001 (4pp), 2025 January
https://doi.org/10.1088/1674-4527/ad9b78
CSTR: 32081.14.RAA.ad9b78

Moderate Influence of Halo Spin on Stellar Mass Distributions in Dwarf and Massive Galaxies

Yu Rong[1,2], Zichen Hua[1,2], and Huijie Hu[3]
[1] Department of Astronomy, University of Science and Technology of China, Hefei 230026, China; rongyua@ustc.edu.cn
[2] School of Astronomy and Space Sciences, University of Science and Technology of China, Hefei 230026, China
[3] University of Chinese Academy of Sciences, Beijing 100049, China
Received 2024 November 11; accepted 2024 November 27; published 2025 January 8

Abstract

We estimate halo spins for H I-rich galaxies in the Arecibo Legacy Fast ALFA survey using a semi-analytic approach, examining the relationship between halo spin and stellar surface density. Our findings reveal an inverse correlation in both low- and high-mass galaxy samples, with stellar surface density decreasing as halo spin increases. This trend highlights the pivotal role of halo spin in galaxy evolution and suggests a universal formation scenario: high-spin halos, accompanied by high-spin accreted gas, retain angular momentum, preventing gas from efficiently condensing in the galactic center and thus suppressing star formation. Consequently, weak feedback redistributes gas to the halo outskirts without significant expulsion. The shallower central gravitational potential in high-spin halos promotes outward stellar migration, leading to more extended stellar distributions and lower stellar surface densities.

Key words: methods: statistical – galaxies: formation – galaxies: evolution

1. Introduction

In empirical models of galaxy formation, galaxy properties are largely determined by the characteristics of their host dark matter halos. Key processes, including gas accretion, temperature, angular momentum retention, and star formation efficiency, are influenced by these halo properties (e.g., Silk 1977; Fardal et al. 2001; Kereš et al. 2005; Behroozi et al. 2010; Rubin et al. 2010, 2015; Guo et al. 2011; van de Voort et al. 2012; Yang et al. 2012; Nelson et al. 2013; Lehner et al. 2014; Girelli et al. 2020; Noguchi 2023). For example, halos with shallower potential wells and lower concentrations exhibit more pronounced feedback effects, which lead to reduced star formation efficiencies, lower stellar mass fractions, and more extended stellar distributions (Hopkins et al. 2012; Sawala et al. 2015; Kravtsov & Vikhlinin 2018; Sales et al. 2022). Based on hydrodynamical simulations, in low-mass halos, gas inflow is dominated by "cold mode" accretion, resulting in subsonic flows that create "hot" structures with more diffuse stellar distributions (Noguchi 2018, 2022; Kalita et al. 2022). In contrast, gas accretion in massive halos occurs through a "hot mode," where supersonic inflows lead to thin, disk-like "cold" structures with significant angular momentum (Noguchi 2018; Hafen et al. 2022).

Despite extensive research, the influence of halo spin on galaxy structure and evolution remains incompletely understood. It is generally accepted that the spin of a dark matter halo impacts the stellar distribution in massive late-type galaxies (Mo et al. 1998; van den Bosch 1998; Diemand et al. 2005; Kim & Lee 2013; Desmond et al. 2017). However, for low-mass galaxies, high-resolution simulations indicate that halo spin may not play as critical a role as it does in massive counterparts, although it may be essential in forming diffuse stellar distributions in ultra-diffuse galaxies (Amorisco & Loeb 2016; Rong et al. 2017; Di Cintio et al. 2019; Benavides et al. 2023; Yang et al. 2023).

To date, research on the effects of halo spin on stellar distributions has been inconclusive, particularly in observational studies where halo spin determination poses significant challenges. Observational halo spin measurements have largely focused on small, high-surface-brightness samples (e.g., Cappellari et al. 2006; Cappellari et al. 2013; Rong et al. 2018; Wang et al. 2020), often introducing selection biases. This limitation complicates efforts to accurately investigate the correlation between halo spin and stellar distribution.

Large H I surveys conducted with single-dish telescopes provide a unique opportunity to obtain H I spectra for a large number of galaxies, offering essential dynamical data to estimate halo spin parameters for H I-rich galaxies. Since these samples are selected based on H I column densities rather than stellar characteristics, they present an unbiased approach for examining the relationship between halo spin and stellar distribution.

In this study, we estimate halo spins for H I-bearing galaxies selected from the Arecibo Legacy Fast ALFA (ALFALFA; Giovanelli et al. 2005; Haynes et al. 2018) survey and analyze their relationship with stellar density. Section 2 describes the

data sample and our approach for estimating halo spin. Section 3 provides a statistical analysis of the correlation between stellar density and halo spin. Our conclusions are summarized and discussed in Section 4.

2. Data

2.1. Galaxy Sample

Our sample is drawn from ALFALFA, an extensive H I survey covering roughly 6600 $\deg^2$ at high Galactic latitudes. The final ALFALFA catalog (α.100; Haynes et al. 2018) includes around 31,500 sources with radial velocities below 18,000 $\mathrm{km\,s^{-1}}$, each characterized by properties such as H I spectrum signal-to-noise ratio (SNR), cosmological distance, H I line 50% peak width of the H I line (W_{50}) corrected for instrumental broadening, and H I mass ($M_{\rm H\,I}$). For definitions of these parameters, uncertainties, and estimation techniques, readers are referred to Haynes et al. (2018).

2.2. Stellar Surface Density

ALFALFA sources have been cross-matched with Sloan Digital Sky Survey (SDSS) data (Alam et al. 2015). Previous studies by Durbala et al. (2020) estimated stellar masses $M_\star$ for ALFALFA galaxies with optical counterparts using three methods: ultraviolet (UV)-optical-infrared spectral energy distribution (SED) fitting, SDSS $g-i$ color, and infrared W_2 magnitude. We prioritize stellar masses derived from SED fitting, using $g-i$ color estimates only where SED fits are unavailable due to missing UV or infrared data. Discrepancies among these estimates are considered negligible.

To compute stellar densities for the ALFALFA galaxies, we require their effective radii $R_{\rm e}$. For approximately 40% of ALFALFA galaxies, effective radii were measured by Du et al. (2019). For the remainder, we cross-match with the Simard et al. (2011) catalog, which provides effective radii for SDSS galaxies. For galaxies without existing radii, we employ the SExtractor software (Bertin & Arnout 1996) to estimate g-band effective radii following the method of Du et al. (2015).

The stellar density $S_\star$ is calculated as $\log S_\star = \log M_\star + 2.5\log(2\pi R_{\rm e}^2)$, with $M_\star$ and $R_{\rm e}$ given in units of $M_\odot$ and kpc, respectively.

2.3. Halo Spin

To estimate halo spin, we first calculate each galaxy's rotation velocity from its H I spectrum, given by $V_{\rm rot} = W_{50}/2/\sin\phi$, where ϕ is the H I disk inclination. When direct H I data are unavailable, we estimate ϕ using the optical axis ratio b/a from Durbala et al. (2020), calculating inclination as $\sin\phi = \sqrt{(1-(b/a)^2)/(1-q_0^2)}$, setting $\phi = 90°$ if $b/a \leqslant q_0$. We use the intrinsic thickness $q_0 \sim 0.2$ for massive galaxies, and $q_0 \sim 0.4$ for low-mass galaxies with $M_\star < 10^{9.5}\,M_\odot$ (Giovanelli et al. 1997; Tully et al. 2009; Li et al. 2022; Rong et al. 2024a).

To improve rotation velocity accuracy, we exclude galaxies with inclinations $\phi < 50°$ or low H I SNRs (SNR < 10) due to higher velocity uncertainties.

For galaxies dominated by velocity dispersion rather than rotation, identified by "single-horned" H I profiles (ElBadry et al. 2018), rotation velocity estimates and thus halo spins are unreliable. To classify single- versus double-horned spectra, we apply the kurtosis parameter k_4, following Hua et al. (2024); spectra with $k_4 > -1.0$ are considered single-horned. This study focuses on isolated galaxies with double-horned profiles to avoid dispersion-dominated sources.

Halo spin $\lambda_{\rm h}$ is then calculated as (Hernandez et al. 2007)

$$\lambda_{\rm h} \simeq 21.8\frac{R_{\rm HI,d}/\mathrm{kpc}}{(V_{\rm rot}/\mathrm{km\ s^{-1}})^{3/2}}, \quad (1)$$

where the H I disk scale length, $R_{\rm H\,I,d}$, is derived assuming a thin gas disk in centrifugal balance (Mo et al. 1998) with an exponential surface density profile

$$\Sigma_{\rm HI}(R) = \Sigma_{\rm HI,0}\exp(-R/R_{\rm HI,d}), \quad (2)$$

where $\Sigma_{\rm H\,I,0}$ is the central H I surface density. The total H I mass $M_{\rm H\,I}$ relates to the scale length by

$$M_{\rm HI} = 2\pi\Sigma_{\rm HI,0}R_{\rm HI,d}^2. \quad (3)$$

We introduce the H I radius $r_{\rm H\,I}$, defined as the radius where H I surface density is $1\,M_\odot\,\mathrm{pc^{-2}}$. $r_{\rm H\,I}$ is estimated using the empirical relation $\log r_{\rm HI} = 0.51\log M_{\rm HI} - 3.59$ (Wang et al. 2016; Gault et al. 2021). At $r_{\rm H\,I}$, we set

$$\Sigma_{\rm HI,0}\exp(-r_{\rm HI}/R_{\rm HI,d}) = 1 \quad M_\odot\ \mathrm{pc^{-2}}. \quad (4)$$

Solving Equations (3) and (4) allows us to compute $R_{\rm H\,I,d}$, enabling robust halo spin estimation for each galaxy in our sample.

3. Results

Our final sample comprises 6680 galaxies with stellar masses spanning 10^7–$10^{11}\,M_\odot$. Panels (a) and (b) of Figure 1 illustrate the relationship between $S_\star$ and $\lambda_{\rm h}$ for the low-mass ($M_\star < 10^9\,M_\odot$) and massive ($M_\star > 10^9\,M_\odot$) galaxies, respectively. The blue and red points with error bars represent the median $\lambda_{\rm h}$ values and their 1σ uncertainties across different $\log S_\star$ bins. A linear fit to these medians yields $\log\lambda_{\rm h} = (-0.09\pm0.09)\log S_\star - (0.16\pm0.59)$ for the low-mass galaxies, and $\log\lambda_{\rm h} = (-0.11\pm0.09)\log S_\star + (0.04\pm0.73)$ for high-mass galaxies. The correlation coefficients of -0.21 and -0.31 suggest a weak correlation in low-mass galaxies and a moderate correlation in high-mass galaxies.

Considering that environmental factors can affect galaxy size and thereby stellar density (Moore et al. 1996; Mayer et al. 2001; Mastropietro et al. 2005; Kazantzidis et al. 2011; Smith

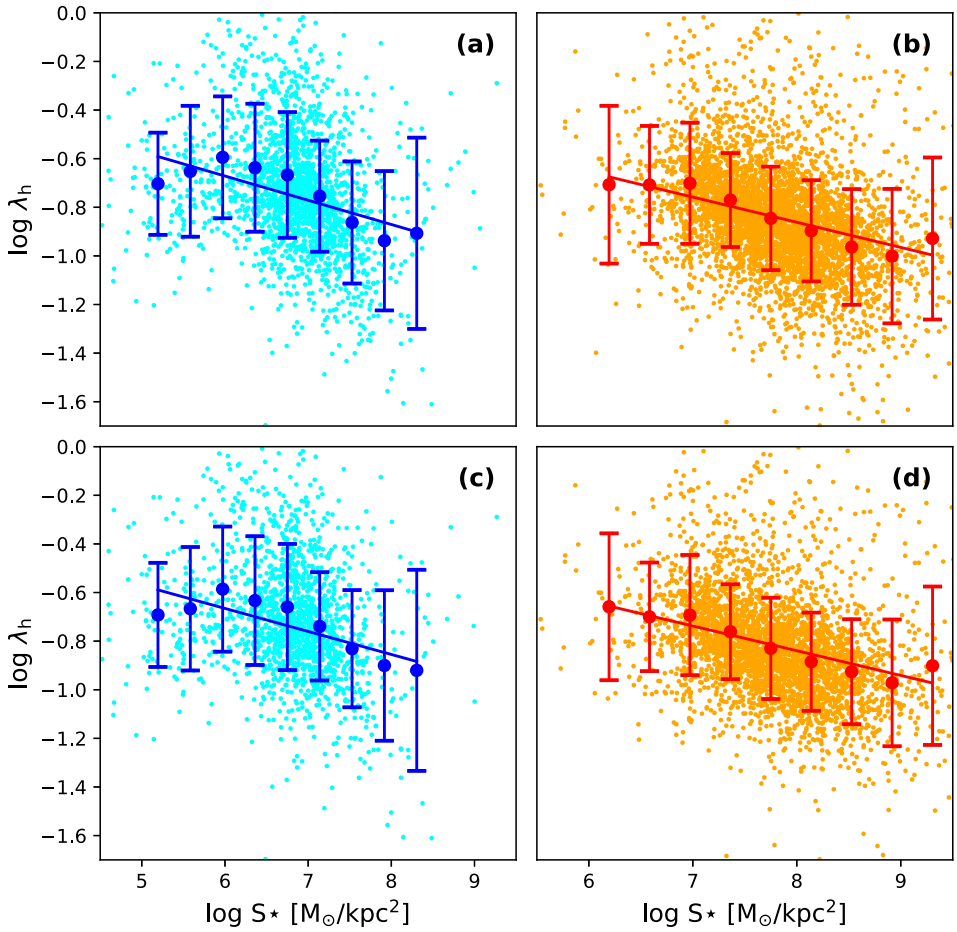

Figure 1. The relationships between stellar surface densities and halo spins for low-mass (left) and massive (right) galaxies. The upper and lower panels correspond to the entire sample and isolated galaxy sample, respectively. Median $\log \lambda_{\rm h}$ values with 1σ error bars are shown in blue and red for bins in $\log S_{\star}$. The best linear fitting results are highlighted by the corresponding lines.

et al. 2015), we control for environmental influences by using the galaxy group catalog from Saulder et al. (2016), constructed with a friends-of-friends algorithm based on SDSS Data Release 12 (DR12) (Alam et al. 2015) and 2MASS Redshift Survey (Huchra et al. 2012) data, accounting for biases like the Malmquist bias and "Fingers of God" effect.

We further refine the sample to include only isolated galaxies, defined as those located more than three times the virial radius from any galaxy group or cluster (Rong et al. 2024b) to minimize effects of tidal stripping and ram pressure stripping (Mamon et al. 2004; Gill et al. 2005; Oman et al. 2013; Zinger et al. 2018). Panels (c) and (d) of Figure 1 display the relationship between $\lambda_{\rm h}$ and $S_{\star}$ for this isolated sample. Linear fits yield $\log \lambda_{\rm h} = (-0.08 \pm 0.09)\log S_{\star} - (0.20 \pm 0.60)$ for isolated low-mass galaxies and $\log \lambda_{\rm h} = (-0.11 \pm 0.09)\log S_{\star} + (0.03 \pm 0.69)$ for isolated high-mass galaxies, with correlation coefficients of -0.18 and -0.30 respectively, indicating the persistence of weak to moderate correlations between $S_{\star}$ and $\lambda_{\rm h}$ across galaxy masses, independent of environmental effects.

4. Summary and Discussion

Using a semi-analytic approach, we estimate halo spin parameters ($\lambda_{\rm h}$) for H I-rich galaxies in the ALFALFA survey and examine how the stellar surface density ($S_{\star}$) varies with halo spin in isolated low- and high-mass samples. Our analysis reveals a moderate correlation between $\lambda_{\rm h}$ and $S_{\star}$ in both galaxy samples, implying that halo spin significantly influences gas cooling, star formation, and feedback processes within galaxies. This finding is consistent with prior results in Rong et al. (2024b) but indicates that the correlation between halo spin and stellar surface density is weaker than that between halo spin and H I-to-stellar mass ratios (Liu et al. 2024).

As proposed by Rong et al. (2024b), high-spin halos acquire gas with high angular momentum, which resists momentum loss and slows its inward motion and cooling. This process restricts the accumulation of cold gas at the galactic center, reducing the fuel for star formation (Peng & Renzini 2020). Consequently, gas inflow and star formation are more gradual, minimizing supernova-driven feedback and limiting gas

expulsion from the halo. Instead, gas is displaced outward within the halo, weakening the central gravitational potential and promoting an extended stellar distribution as stars and dark matter migrate outward (Di Cintio et al. 2017; Yang et al. 2024). Our results suggest that this halo-spin-dependent formation scenario may apply universally across galaxy types.

However, the weaker correlation observed between $\lambda_{\rm h}$ and $S_\star$ compared to that between $\lambda_{\rm h}$ and H I-to-stellar mass ratios (Liu et al. 2024) suggests that stellar distribution may also be shaped by additional mechanisms beyond halo spin alone, indicating a more complex set of processes at work in galaxy evolution.

Note that we utilize a semi-analytic method to estimate the halo spin, which may introduce relatively large uncertainties. For example, the application of Equation (1) relies on the assumption of spherically symmetric dark matter halo systems, a universally applicable baryonic Tully–Fisher relation with a slope of 3.5, and the same specific angular momenta of cool gas and halo. The assumed geometry and kinematics of the cool gas disk may also be overly idealized. As a result, the estimated spins from Equation (1) are statistically higher than those of dark matter halos in simulations (e.g., Bett et al. 2007). However, since the spins of both galaxy samples with low and high stellar surface densities are likely overestimated, the correlation between $\lambda_{\rm h}$ and $S_\star$ cannot be attributed to spin overestimation. Nevertheless, this relationship underscores the robust correlation between the two galaxy characteristics, and further observational investigations are warranted to re-examine the moderate correlation between them.

Acknowledgments

We thank Min He and Wei Du for help on photometry. Y.R. acknowledges supports from the CAS Pioneer Hundred Talents Program (Category B), and the National Natural Science Foundation of China (NSFC, grant No. 12273037), as well as the USTC Research Funds of the Double First-Class Initiative. This work is also supported by the research grants from the China Manned Space Project (the second-stage CSST science projects: "Investigation of small-scale structures in galaxies and forecasting of observations" and "CSST study on specialized galaxies in ultraviolet and multi-band"). H.H. is supported by the China Postdoctoral Science Foundation grant No. 2024M763213.

References

Alam, M. P., Albareti, F. D., Allende Prieto, C., et al. 2015, ApJS, 219, 12
Amorisco, N. C., & Loeb, A. 2016, MNRAS, 459, l51
Behroozi, P. S., Conroy, C., & Wechsler, R. H. 2010, ApJ, 717, 379
Benavides, J. A., Sales, L. V., Abadi, M. G., et al. 2023, MNRAS, 522, 1033
Bertin, E., & Arnouts, S. 1996, A&AS, 117, 393
Bett, P., Eke, V., Frenk, C.S., et al. 2007, MNRAS, 376, 215
Cappellari, M., Bacon, R., Bureau, M., et al. 2006, MNRAS, 366, 1126
Cappellari, M., McDermid, R. M., Alatalo, K., et al. 2013, MNRAS, 432, 1862
Desmond, H., Mao, Y.-Y., Wechsler, R. H., Crain, R. A., & Schaye, J. 2017, MNRAS, 471, L11
Di Cintio, A., Brook, C. B., Dutton, A. A., et al. 2017, MNRAS, 466L, L1
Di Cintio, A., Brook, C. B., Macciò, A. V., Dutton, A. V., & Cardona-Barrero, S. 2019, MNRAS, 486, 2535
Diemand, J., Madau, P., & Moore, B. 2005, MNRAS, 364, 367
Du, W., Cheng, C., Wu, H., Zhu, M., & Wang, Y. 2019, MNRAS, 483, 1754
Du, W., Wu, H., Lam, M. I., et al. 2015, AJ, 149, 199
Durbala, A., Finn, R. A., Crone Odekon, M., et al. 2020, AJ, 160, 271
El-Badry, K., Quataert, E., Wetzel, A., et al. 2018, MNRAS, 473, 1930
Fardal, M. A., Katz, N., Gardner, J. P., et al. 2001, ApJ, 562, 605
Gault, L., Gressier, A., Wright, S., et al. 2021, AJ, 909, 19
Gill, S. P. D., Knebe, A., & Gibson, B. K. 2005, MNRAS, 356, 1327
Giovanelli, R., Haynes, M. P., Kent, B. R., et al. 2005, AJ, 130, 6
Giovanelli, R., Haynes, M. P., Herter, T., et al. 1997, AJ, 113, 22
Girelli, G., Pozzetti, L., Bolzonella, M., et al. 2020, A&A, 634, A135
Guo, Q., White, S., Boylan-Kolchin, M., et al. 2011, MNRAS, 413, 101
Hafen, Z., Stern, J., Bullock, J., et al. 2022, MNRAS, 514, 5056
Haynes, M. P., Giovanelli, R., Kent, B. R., et al. 2018, ApJ, 861, 49
Hernandez, X., Park, C., Cervantes-Sodi, B., & Choi, Y.Y. 2007, MNRAS, 375, 163
Hopkins, P. F., Quataert, E., & Murray, N. 2012, MNRAS, 421, 3488
Hua, Z., Rong, Y., & Hu, H.J. 2024, arXiv:2403.16754
Huchra, J. P., et al. 2012, ApJS, 199, 26
Kalita, B. S., Daddi, E., Bournaud, F., et al. 2022, A&A, 666A, 44
Kazantzidis, S., Lokas, E., Callegari, S., Mayer, L., & Moustakas, L. 2011, ApJ, 726, 98
Kereš, D., Katz, N., Weinberg, D.H., & Davé, R. 2005, MNRAS, 363, 2
Kim, J.H., & Lee, J. 2013, MNRAS, 432, 1701
Kravtsov, A. V., & Vikhlinin, A. A. 2018, AstL, 44, 8
Lehner, N., O'Meara, J.M., Fox, A.J., et al. 2014, ApJ, 788, 119
Li, X., Shi, Y., Zhang, Z.-Y., et al. 2022, MNRAS, 516, 4220
Liu, S., Rong, Y., Hua, Z., & Hu, H. 2024, arXiv:2411.11446
Mamon, G. A., Sanchis, T., Salvador-Solé, E., & Solanes, J. M. 2004, A&A, 414, 445
Mastropietro, C., Moore, B., Mayer, L., et al. 2005, MNRAS, 364, 607
Mayer, L., Governato, F., Colpi, M., et al. 2001, ApJ, 547, L123
Mo, H. J., Mao, S. D., & White, S. D.M. 1998, MNRAS, 295, 319
Moore, B., Katz, N., Lake, G., et al. 1996, Natur, 379, 613
Nelson, D., Vogelsberger, M., Genel, S., et al. 2013, MNRAS, 429, 3353
Noguchi, M. 2018, Natur, 559, 585
Noguchi, M. 2022, MNRAS, 510, 1772
Noguchi, M. 2023, MNRAS, 522, 4691
Oman, K. A., Hudson, M. J., & Behroozi, P. S. 2013, MNRAS, 431, 2307
Peng, Y.-J., & Renzini, A. 2020, MNRAS, 491L, 51
Rong, Y., Guo, Q., Gao, L., et al. 2017, MNRAS, 470, 4231
Rong, Y., et al. 2018, MNRAS, 477, 230
Rong, Y., He, M., Hu, H., Zhang, H.X., & Wang, H.Y. 2024a, arXiv:2409.00944
Rong, Y., Hu, H., He, M., et al. 2024b, arXiv:2404.00555
Rubin, K. H., Hennawi, J. F., Prochaska, J. X., et al. 2015, ApJ, 808, 38
Rubin, K. H., Prochaska, J. X., Koo, D. C., Phillips, A. C., & Weiner, B. J. 2010, ApJ, 712, 574
Sales, L. V., Wetzel, A., & Fattahi, A. 2022, NatAs, 6, 897
Saulder, C., van Kampen, E., Chilingarian, I.V., Mikske, S., & Zeilinger, W.W. 2016, A&A, 596, A14
Sawala, T., Frenk, C. S., Fattahi, A., et al. 2015, MNRAS, 448, 2941
Silk, J. 1977, ApJ, 211, 638
Simard, L., Mendel, J. T., Patton, D. R., Ellison, S. L., & McConnachie, A. W. 2011, ApJS, 196, 11
Smith, R., Sánchez-Janssen, R., Beasley, M. A., et al. 2015, MNRAS, 454, 2502
Tully, R. B., Rizzi, L., Shaya, E. J., et al. 2009, AJ, 138, 323
van de Voort, F., Schaye, J., Altay, G., & Theuns, T. 2012, MNRAS, 421, 2809
van den Bosch, F.C. 1998, ApJ, 507, 601
Wang, B., Cappellari, M., Peng, Y., & Graham, M. 2020, MNRAS, 495, 1958
Wang, J., Koribalski, B.S., Serra, P., et al. 2016, MNRAS, 460, 2143
Yang, H., Gao, L., Frenk, C. S., et al. 2023, MNRAS, 518, 5253
Yang, H., Liao, S., Fattahi, A., et al. 2024, MNRAS, 535, 1394
Yang, X., Mo, H.J., van den Bosch, F.C., Zhang, Y., & Han, J. 2012, ApJ, 752, 41
Zinger, E., Dekel, A., Kravtsov, A. V., & Nagai, D. 2018, MNRAS, 475, 3654